Room temperature photoluminescence of (RE)NiO$_3$ (RE=La, Y, Er, Ho, Nd and La$_{1-x}$Y$_x$)

(Fotoluminescência à temperatura ambiente de (TR)NiO$_3$ (TR=La, Y, Er, Ho, Nd e La$_{1-x}$Y$_x$))

Z. R. Silva[1], D. M. A. Melo[1], A. C. Lima[1], E. Longo[2], M. A. F. Melo[1], A. E. Martinelli[3]
[1]*Department of Chemistry, URFN, Natal, RN, P.O. Box 1662, Natal, RN, Brazil 59078-970*
[2]*Department of Chemistry, UFSCar, P.O. Box 676, S. Carlos, SP, Brazil 13565-905*
[3]*Department of Materials Engineering, URFN, P.O. Box 1662, Natal, RN, Brazil 59078-970*
dmelo@matrix.com.br, tel./fax: +55-84-3211-9241

Abstract

The nature of visible photoluminescence (PL) at room temperature in amorphous (RE)NiO$_3$ (RE=La, Y, Er, Ho, Nd and La$_{1-x}$Y$_x$) is discussed. Powders of this system were prepared by the polymeric precursor technique. The presence of broad PL band emission spectra at room temperature indicated increasing structural order with addition of rare earth elements.
Keywords: sol-gel process, photoluminescence, rare earths.

Resumo

É discutido o fenômeno da fotoluminescência à temperatura ambiente observada em compostos amorfos do tipo (TR)NiO$_3$ (TR = La, Y, Er, Ho, Nd e La$_{1-x}$Y$_x$). Pós com essas composições foram preparados a partir de precursores poliméricos. A presença de uma banda de emissão fotoluminescente larga à temperatura ambiente está associada ao aumento da ordenação estrutural com a adição de íons de terras raras ao sistema.
Palavras-chave: *processo sol-gel, fotoluminescência, terras raras.*

INTRODUCTION

ABO$_3$ perovskites are important ferroelectric materials used for different applications in electronic technology [1, 2]. Their optical properties, such as luminescence, especially in nanostructured powders, have attracted considerable attention in the past few years [3-5]. In particular, photoluminescence (PL), is a sensitivity tool to assess energy levels of materials, rarely defined by absorption measurements [6]. Such levels are responsible for storing energy before emission occurs [7, 8]. The combination of absorption and photoluminescence excitation measurements provides fundamental information on the properties of energy levels lying within the band gap of the material [9]. The luminescence of ABO$_3$ structures has been materials well established. The phenomenon has been observed at room temperature either in crystalline materials or in pure samples excited by radiation above the band gap energy [3]. In perovskite-type crystals, a broad luminescence band associated to the presence of material imperfections or defects is usually observed at low temperatures [10]. Such behavior has renewed the interest in the luminescent properties of nickelate semiconductors. Amorphous semiconductors, such as LaNiO$_3$ and YNiO$_3$,

appear to be especially promising materials, since their structure display numerous imperfections and can be synthesized at low temperatures by chemical routes, such as the sol-gel process. Many reports have been published on the luminescence of perovskite–type compounds having either bulk or nanometric crystalline structures [11, 12]. Nonetheless, little or no information is available on the behavior of disordered perovskite-type compounds. PL is an effective characterization technique capable of providing simultaneous information on both shallow and deep level defects as well as gap-states of a variety of semiconductors [13]. Room temperature PL occurs due to structural disorder presents in these compounds. Should the system be totally disordered or, conversely, fully ordered, PL is not observed [14]. Some degree of order is necessary so the material can exhibit PL. Amorphous metal oxides synthesized by the polymeric precursor method display intense PL at room temperature. A simple water-based chemical process has been used, allowing amorphous metal oxide particles to be synthesized at temperatures as low as 300 °C. In fact, this method has been used to synthesize nanoparticles of several materials. It is based on the chelation of cations by a carboxylic acid, such as citric acid, in aqueous solution.

However, despite extensive studies, only recently room temperature PL has been reported for amorphous powders and thin films [15, 16]. In the present study, efficient room-temperature PL is reported for amorphous $(RE)NiO_3$ (RE=La, Y, Er, Ho, Nd, and $La_{1-x}Y_x$) powders prepared by the polymeric precursor method [17, 18]. PL measurements were taken to study order-disorder transitions in $(RE)NiO_3$ perovskite-type compounds submitted to calcination. This investigation did not focus on the effect of the temperature. Instead, emphasis was given on the influence of the rare earth ion on the increase of structural order of the solid solution.

EXPERIMENTAL

Amorphous $(RE)NiO_3$ (RE=La, Y, Er, Ho, Nd, and $La_{1-x}Y_x$) powders, for $x = 0, 0.2, 0.6, 0.9$ and 1.0, were prepared by a sol-gel method from polymeric precursors. The method is based on the chelation of metallic cations by citric acid in aqueous solution, followed by the addition of ethylene glycol. Nickel citrates were formed by the dissolution of $Ni(NO_3)_2$ in citric acid aqueous solution at 60-70 °C. After homogenization of the Ni citrate solution, ethylene glycol was slowly added to promote the polymerization of the mixed citrates by polyesterification between 90 and 120 °C, followed by water removal. The citric acid:ethylene glycol molar ratio was set to 60:40. The resulting polyester resin was annealed at 300 °C for 4 h to obtain a powder, which was crushed and pre-calcined at 300 °C for 4 h under flowing oxygen to promote the oxidation of organic matter and pre-pyrolysis without crystallization. The $(RE)NiO_3$ powders were subsequently calcined at 750 °C for 2 h.

The evolution of the gel system with temperature was investigated by thermogravimetric analysis (TGA) in synthetic air flowing at 50 cm^3.min^{-1}. The heating rate from room temperature to 1000 °C was set to 5 °C.min^{-1}. X-ray diffraction (XRD) patterns of the synthesized materials were obtained using CuK$_\alpha$ radiation in order to determine the structure of the powders. Photoluminescence spectra were obtained using a U1000 Jobin-Yvon double monochromator coupled to a cooled GaAs photomultiplier and a conventional photon counting system. The 488.0 nm line of an argon ion laser was used as excitation light. The maximum output power of the laser was kept between 100 and 200 mW. Cylindrical lenses were used to prevent sample overheating. All measurements were taken at room temperature.

RESULTS AND DISCUSSION

The X-ray diffraction patterns of $La_{1-x}Y_xNiO_3$ powders calcined at different temperatures are shown in Fig. 1. Samples calcined at lower temperatures were amorphous, whereas those treated at 750 °C displayed patterns characteristic of crystalline materials. On the hand, with increasing the calcination temperature, adsorbed Ni^{3+} became unstable, and the reduction of Ni^{3+} to Ni^{2+} occurred. This scenario was associated to the presence of impure NiO and Y_2O_3 observed in the XRD pattern shown in Fig.
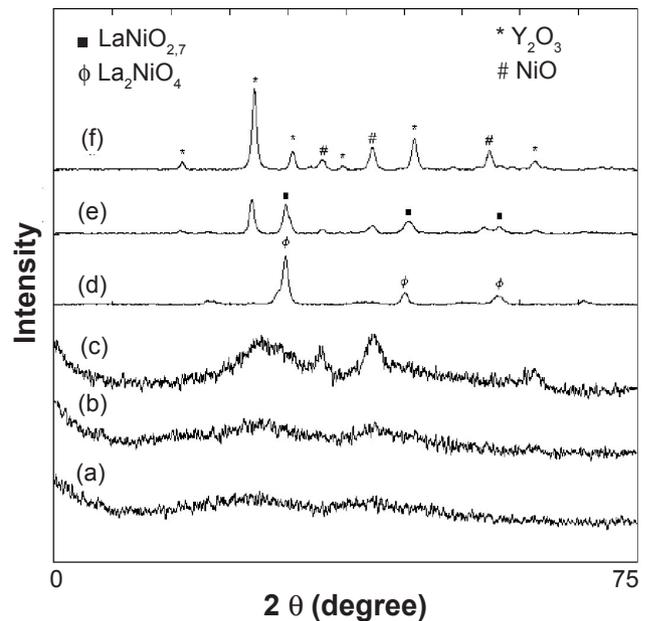

Figure 1: X-ray diffraction patterns of $La_{1-x}Y_xNiO_3$. (a) x=0.2, (b) x=0.6 and (c) x= 0.9 calcined at 300 °C. (d) x= 0.2, (e) x= 0.6 and (f) x= 0.9 calcined at 750 °C.
[Figura 1: Difratogramas de raios X do $La_{1-x}Y_xNiO_3$. (a) x=0,2, (b) x=0,6 and (c) x= 0,9 calcinado a 300 °C. (d) x= 0,2, (e) x= 0,6 e (f) x= 0,9 calcinado a 750 °C.]

1f [19]. All the peaks were ascribed to a cubic perovskite structure. In addition, thermogravimetric analyses of the powders revealed no weight loss after calcination for 4 h at 300 °C under flowing oxygen. These results suggested that an inorganic amorphous material was formed.
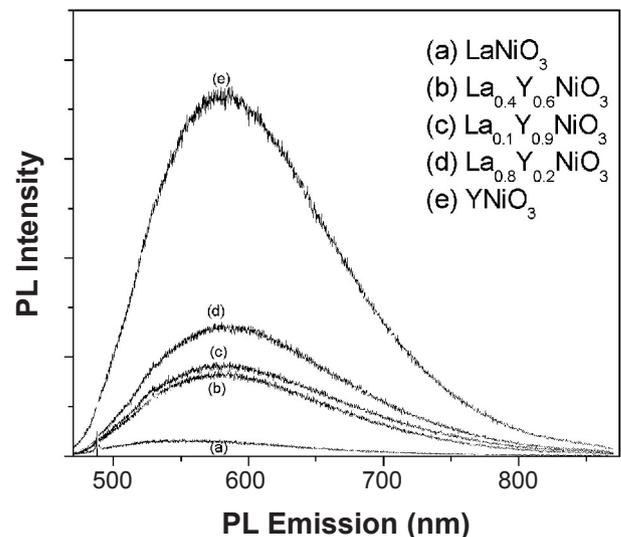
Experimental PL curves obtained at 300 K for $LaNiO_3$,

Figure 2: Photoluminescence spectra of amorphous (a) $LaNiO_3$ and $La_{1-x}Y_xNiO_3$, where (b) x = 0.6 , (c) 0.9 , (d) 0.2 and (e) $YNiO_3$.
[Figura 2: Espectros de fotoluminescência de pós amorfos de (a) $LaNiO_3$ e $La_{1-x}Y_xNiO_3$, onde (b) x = 0,6 , (c) 0,9 , (d) 0,2 e (e) $YNiO_3$).]
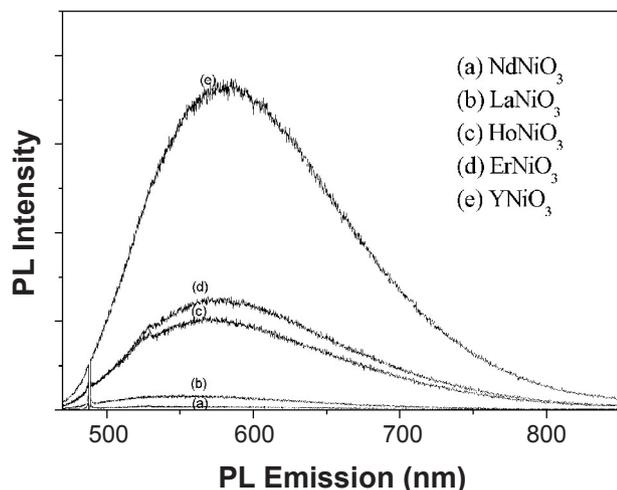
Figure 3: Photoluminescence spectra of amorphous (a) $NdNiO_3$ (NN), (b) $LaNiO_3$ (LN), (c) $HoNiO_3$ (HN), (d) $ErNiO_3$ (EN) and (e) $YNiO_3$ (YN).

[Figura 3: Espectros de fotoluminescência de pós amorfos de (a) $NdNiO_3$ (NN), (b) $LaNiO_3$ (LN), (c) $HoNiO_3$ (HN), (d) $ErNiO_3$ (EN) e (e) $YNiO_3$ (YN).]

$YNiO_3$ and $La_{1-x}Y_xNiO_3$ (x = 0.2, 0.6 and 0.9) are illustrated in Fig. 2. The PL behavior of amorphous phases is quite noticeable, since the spectra corresponding to yttrium and lanthanum nickelates were predominantly characterized by a broad band in the visible region. The photoluminescence spectra of $ErNiO_3$ (EN), $HoNiO_3$ (HN), $NdNiO_3$ (NN), $LaNiO_3$ (LN) and $YNiO_3$ (YN) compounds were all rather similar with the presence of a roadand intense band at room temperature. The spectra of all five materials excited by the 488.0 nm line are displayed in Fig. 3. All maximum peak positions were around 570 nm.

To rationalize the behavior observed, it is important to consider the structural organization that takes place along the synthesis process. When in solution, the nickel ion is chelated by citric acid, forming nearly regular NiO_6 clusters without constraints. These are surrounded by a random distribution of network modifier rare earth ions, yielding some organization. When the solution is polymerized, this organization is set in rigid 3D networks. The Ni-O coordination is nearly regular with little deformation due to the cubic distortion. Such a distortion is related to the nature of the network modifier. For example, La forms cubic perovskite structures because of its stronger ionic character compared to Y. The size of its electronic cloud is responsible for the structural deformation. As the gel is calcined, organic compounds are eliminated, but the local order (NiO_6) is maintained. Complete crystallization is achieved as long range organization occurs in addition to local order, which may deviate from the ideal structure due to constrains induced by the long range order.

(RE)NiO_3 are interesting compounds to study PL, due to order-disorder transitions. Ordering or disordering of (RE)NiO_3, with corresponding change in PL, can be obtained depending on the rare earth element added. In

contrast with the almost regular NiO_6 octahedra observed in (RE)NiO_3 for large rare earth ions (La or Nd) [20], increasing distortion is observed in the NiO_6 octahedra from $SmNiO_3$ to $DyNO_3$. This distortion is still more pronounced for $YNiO_3$ and $HoNiO_3$, in which the two different kinds of NiO_6 octahedra are fairly distorted. It is belived that no anisotropy could be detected in NiO_6 octahedra for large rare-earth cations (La or Nd) because of the strong covalent character of Ni-O bonds. The progressive reduction of their covalent contribution along the series explains the increased anisotropy of NiO_6 octahedra as a consequence of the manifestation of Jahn-Teller induced distortions. In this context, it is important to underline that the existence of Jahn-Teller polarons in stoichiometric charge-transfer (RE)NiO_3 systems has been recently demonstrated for lighter rare-earths [21, 22]. This strongly supports the polaronic picture suggested for other perovskite oxides containing JT transition-metal cations [23, 24].

The origin of luminescence has been thoroughly discussed. Suggested mechanisms include donor-acceptor recombination [25], recombination of electron-hole polarons, charge-transfer vibronic excitons [26] and transitions in MeO_6 complexes [27]. However, by first-principle calculations, it can be suggested that the formation of five-fold coordination by the displacement or rotation of the oxygen in the TiO_6 cluster may introduce delocalized electronic levels between the valence and conduction band (energy gap). The coexistence of TiO_6 and TiO_5 coordination in the same amorphous material, with different net cluster charges, induces the formation of a charge gradient, allowing trapping of holes in the new localized electronic levels, responsible for the PL behavior [15, 16]. This finding is a good indication that PL in amorphous powders obtained by the polymeric precursor method stems from inorganic disordered phases. Different optical properties are ascribed to a difference in trapping coordination, NiO_5- and NiO_6-type, symmetry, and longer bond lengths, enhancing excitation trapping in amorphous perovskites. A slight increase in the calcination temperature causes the sample to crystallize, as revealed by Raman spectra (not shown) with concomitant disappearance of PL.

CONCLUSIONS

Intense room temperature PL was observed in highly disordered amorphous $ErNiO_3$, $HoNiO_3$, $NdNiO_3$, $LaNiO_3$ and $YNiO_3$ powders synthesized by the polymeric precursor method. The PL spectra of these materials are quite similar in shape, presenting broad bands in the visible region. The origin of PL might be ascribed to the disordered perovskite structure displayed by these materials.

ACKNOWLEDGEMENTS

REFERENCES

[1] R. N. Schwartz, B. A. Wechsler, L. West, Appl. Phys. Lett. **67** (1995) 1352.

[2] I. H. Parker, B. A. Tasch, IEEE Circuits Devices Mg **6** (1990) 17.

[3] P. C. Joshi, S. B. Desu, Thin Solid Films **300** (1997) 289.

[4] W. F. Zhang, Z. Yin, M. S. Zhang, Appl. Phys. A **70** (2000) 93.

[5] T. Takagahara, K. Takeda, Phys. Rev. B **46** (1992) 15578.

[6] R. K. Willardson, A. C. Beer, Semiconductor and Semimetals, vol. 8, Academic Press, New York (1972) pp.181 and 321.

[7] K. K. Rebane, Impurity of Solids, Plenum Press, New York (1970) p.26.

[8] C. C. Klick, J. H. Schulman, Solid State Phys. **5** (1957) 100.

[9] F. Montoncello, M. C. Capotla, B. Cavicchi, M. Ferroni, A. Giberti, V. Guidi, C. Nalagi, G. Martinelli, F. Meinardi, J. Appl. Phys. **94**, 3 (2003) 1501.

[10] W. F. Zhang, Z. Yin, M. S. Zhang , Z. L. Du, W. C. Cheng, J. Phys. **11** (1999) 5655.

[11] J. Meng, Y. Huang, W. Zhang, Z. Du, Z. Zhu, G. Zou, Phys Lett. A **205** (1995) 72.

[12] A M. Van de Craates , G. J. Dirksen ,G. Blasse, J. Solid State Chem. **118** (1995) 337.

[13] D. K. Schroder, Semiconductor Materials and Device Characterization, John Wiley, New York (1999) p. 490.

[14] P. S. Pizani, E. R. Leite, F. M. Pontes, E. C. Paris, J. H. Rangel, E. Lee, E. Longo, P. Delega, J. A. Varela, Appl. Phys. Lett. **77** (2000) 824.

[15] F. M. Pontes, E. Longo, E. R. Leite, J. A. Varela, Thin Solid Films **386** (2001) 91.

[16] F. M. Pontes, E. Longo, E. R. Leite, E. J. H. Lee, J. A. Varela, P. S. Pizani, C. E. M. Campos, F. Lanciotti, V. Mastellaro, C. D. Pinheiro, Mat. Chem. Plys. **77** (2002) 598.

[17] F. M. Pontes, C. D. Pinheiro, E. Longo, E. R. Leite, S. R. Lazaro, R. Maynani, P. S. Pizani, T. M. Boshi, F. Lanciotti, J. Lumin. **104** (2003) 175.

[18] Z. R. da Silva, J. D. G. Fernandes, D. M. A. Melo, C. Alves Jr, E. R. Leite, C. A. Paskocimas, E. Longo, M. I. B. Bernardi, Mater. Lett. **56** (2002) 232.

[19] Y. Liu, N. Xu, X. G. Zheng, T. Watanabe, O. Agyeman, M. Akiyama, J. Mater. Sci. **35** (2000) 937.

[20] J. L. Garcia-Munõz, J. Rodrigues-Carvajal, P. Lacorre, J. B. Torrance, Phys. Rev. B **46** (1992) 4414.

[21] M. Medarde, P. Lacorre, K. Conder, F. Fauth, A. Furrer, Phys. Rev. Lett. **80**, 11 (1998) 2397.

[22] N. E. Massa, J. A. Alonso, M. J. Martinez-Lope, Phys. Rev. B **56** (1998) 986.

[23] G. M. Zhao, K. Conder, H. Keller, K. A. Muller, Nature **381** (1996) 676.

[24] J. M. de Teresa, M. R. Ibarra, P. A. Algarabel, C. Ritter, C. Blasco, J. Garcia, A. del Moral, Z. Arnold, Nature **386** (1997) 256.

[25] F. M. L. Pontes, E. Longo, E. R. Leite, E. J. H. Lee, J. A. Varela, P. S. Pizani, C. E. M. Campos, F. Lanciotti, V. Mastellaro, C. D. Pinheiro, Mater. Chem. Phys. **77** (2002) 598.

[26] F. M. Pontes, C. D. Pinheiro, E. Longo, E. R. Leite, S. R. Lazaro, J. A. Varela, P. S. Pizani, T. M. Boschi, F. Lanciotti, Mater. Chem. Phys. **78** (2002) 227.

[27] F. M. Pontes, C. D. Pinheiro, E. Longo, E. R. Leite, S. R. Lazaro, R. Magnani, P. S. Pizani, T. M. Boschi, F. Lanciotti, J. Lumin. **104**, 3 (2003) 175.